IEEE Access
Multidisciplinary | Rapid Review | Open Access Journal

Received June 12, 2019, accepted July 5, 2019, date of publication July 15, 2019, date of current version August 12, 2019.

Digital Object Identifier 10.1109/ACCESS.2019.2928883

Modeling of Acoustic Emission Generated by Filter Capacitors in HVDC Converter Station

RUI WANG[1], WENJIE CHEN[1], LINGYU ZHU[1], (Member, IEEE), SHENGCHANG JI[1], XIAOTENG LI[2], LIYU DAI[1], AND YANG YANG[1]

[1]Department of Electrical Engineering, Xi'an Jiaotong University, Xi'an 710049, China
[2]State Grid Shaanxi Electric Power Research Institute, Xi'an 710054, China

Corresponding author: Lingyu Zhu (zhuly1026@mail.xjtu.edu.cn)

This work was supported by the National Natural Science Foundation of China under Project U1766223.

ABSTRACT The acoustic noise generated by filter capacitors in a high voltage direct current (HVDC) converter station will have a serious negative impact on the residents' lives and the ecological environment. Though accurate enough, traditional modeling methods based on either boundary element method (BEM) or finite element method (FEM) are almost impossible to reconstruct sound field for whole HVDC station filter array because of their extremely high demand for computing resources. To deal with this problem, this paper proposes a novel Tikhonov Regularization Equivalent Source Method (TRESM)-based filter capacitor acoustic model. By constructing multiple point-sound source models, the acoustic characteristics of the actual filter capacitor are simulated and the original sound field is reconstructed. The accuracy of the proposed model is verified by the experimental results and the sound field distribution characteristics of the three-phase filter capacitor array are observed and analyzed using the proposed model.

INDEX TERMS Acoustic noise, filter capacitor, modeling, TRESM, HVDC transmission.

I. INTRODUCTION

As we know, the distribution of China's energy resources is extremely uneven. In order to alleviate energy conflicts, high voltage direct current (HVDC) transmission technology has been developed very quickly [1], [2]. However, high-frequency harmonics are generated at the DC side of converter. Therefore, large amount of filter capacitors and reactors are used to eliminate those harmonics, as shown in figure.1. Driven by electromagnetic forces containing high proportions of harmonics, filter capacitors and reactors vibrate at the same time. Which in turn, cause serious acoustic noise pollution. Acoustic noise generated by the filter reactors can reach 70-90dB, and filter capacitors can even generate acoustic noise up to 105dB (after A-Weighting processing) [3], [4]. Compared with other major noise source equipment in the converter station, filter equipment covers a large area and is usually closer to the station boundary, so it has a greater impact on the environment outside. Those kinds of noise can interfere with people's rest and sleep, damage human nervous system, and seriously affect the physical and mental health of the converter station staff as well as surrounding residents [5], [6]. Therefore, it is of great research value to study the characteristics of the filter capacitor sound field and find effective method to reduce such kind of noise.

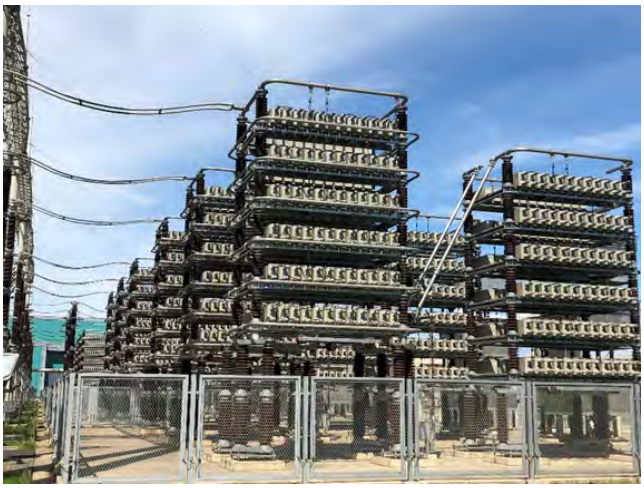

FIGURE 1. Filter capacitors in converter station.

Nowadays, researchers have conducted a lot of research on the noise of filter capacitors. These studies are mainly divided into three aspects, as shown in Figure 2. One is to explore the vibration mechanism of the filter capacitor, and

The associate editor coordinating the review of this manuscript and approving it for publication was Giambattista Gruosso.

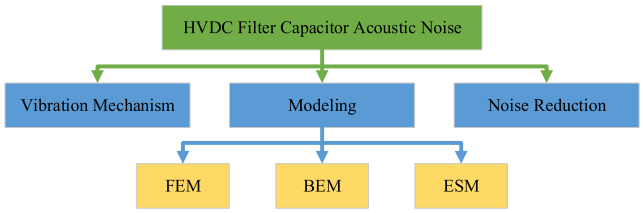

FIGURE 2. Research around HVDC filter capacitor acoustic noise.

obtain the vibration model as well as frequency response function according to the vibration mechanism. The second is to establish acoustic model to analyze the sound field characteristics of the filtering device. The third one is to design the noise reduction method of the filtering device according to the sound field characteristics.

For the vibration mechanism and frequency response function, the capacitor vibration problem was first discovered by M.D.Cox. In [7], he reported that the vibration noise is generated from the electrostatic force between the plates of the capacitor element. In [8], a formula is used to describe the force of the capacitor and analyze the frequency characteristics of the capacitor noise. Cui Xin and etc. obtained the vibration mode of a single capacitor by means of mechanical excitation. They found the natural frequency of the first-order mode at several hundred Hz, which is also confirmed by frequency characteristic analysis results in [9], [10]. And a black box model is introduced to describe the relationship between excitation and vibration response of the filtering device in [11].

These researches show the mechanism of the generation and propagation of capacitor vibration noise, which is fundamental. For the study of sound field characteristics, it is of high academic value.

For noise reduction, traditional methods of noise reduction can be divided into internal measures and external measures. Internal measures suppress the generation of noise. External measures block the spread of noise through sound insulation and vibration reduction [12], [13]. Although the increase of the sound barrier can reduce the noise to a certain extent, the cost will also increase significantly. Besides, it is not conducive to heat dissipation. This will cause new problems in equipment inspection.

As for acoustic modeling and sound field characteristics, boundary element methods (BEM) and finite element methods (FEM) are generally used to analyze field characteristics. In [14], a capacitor model is established by BEM and the results of capacitor elements force analysis are used as boundary condition to simulate the radiation field distribution of a single capacitor. Without taking complex influencing factors into consideration, the simulation results are quite different from the measured results. Moreover, the filtering device covers a large area and consists of a large number of co-frequency sound sources. The model can be improved more and more accurately, but at the same time the computing resources required to complete the solution are greatly improved. A BEM problem with degree of freedom N always needs calculation more than o(N^2), which makes it almost impossible to solve the sound field of whole filter area with more than 2500 capacitors. Simplification of the model will play an important role in this issue. Line source is used to replace the complex capacitor device in [15] for the first time. The model established using line source is greatly simplified. However, it does not consider the interaction of the sound field between the capacitors. So the simulation results are not satisfactory in accordance with the actual results.

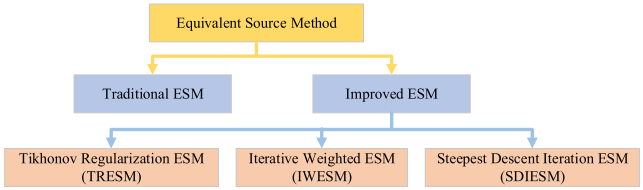

FIGURE 3. Development of equivalent source method.

For the equivalent source method (ESM), The main challenge is to determine the source strength when using traditional ESM. Nowadays, ESM has improved a lot to solve this problem, such as Tikhonov regularization ESM (TRESM), iterative weighted ESM (IWESM) and steepest descent iteration ESM (SDIESM), as shown in Figure 3. TRESM is adopted to solve the ill-posed morbid equation to determine the equivalent source strength accurately [16]. In [17], [18], IWESM is proposed based on the traditional ESM where a weighting matrix was introduced to solve source strength of higher precision. In [19], the steepest descent method was directly used to solve the source strength in SDIESM.

However, due to the complex feature of Lorentz force induced capacitor array acoustic noise, there is a lack of throughout study for this kind of sound field. The motivation of this paper is to propose a new acoustic model based on TRESM to predict the acoustic noise generated by HVDC filter capacitor. The main contributions of this paper are listed as follow.

(1) A novel Tikhonov Regularization Equivalent Source Method (TRESM) based HVDC filter capacitor acoustic model is proposed in this paper. The proposed model uses the superposition of the sound fields generated by the monopole source to approximate the sound field of the original sound source. Certain number of Tikhonov regularization equivalent sources instead of capacitors are used to reconstruct the sound field. It is a great simplification of the traditional acoustic model. Computational resource required for sound field simulation are reduced significantly. Moreover, TRESM could increase computational efficiency, which provides a feasible method for wide-area sound field acoustic solution.

(2) The proposed TRESM based simulation results are compared with the experimental results as well as the BEM based simulation results. The acoustic experimental measurement for an industrial high voltage oil-immersed full-film filter capacitor with length 380mm width 145mm height 380mm is carried out in semi-anechoic chamber. It can be

seen the sound field of the filter capacitor can be predicted accurately when frequency is lower than 1300Hz.

(3) Based upon the proposed mode, sound field distribution characteristics of three-phase filter capacitor array are observed. Simulation results of traditional BEM based model and the proposed TRESM based HVDC filter capacitor acoustic model are also compared. It is found the proposed model is much more effective, adaptive and feasibly.

This paper is organized as follows. In section II, mechanism of filter capacitor vibration and noise is introduced. In section III, modeling process of the TRESM model is introduced and an TRESM based filter capacitor acoustic model is proposed. The sound field is reconstructed and observed in Virtual. Lab, and results are compared with the reconstructed sound field obtained by BEM model. To verify the accuracy and reliability of the proposed TRESM model, experimental measurement is carried out in semi-anechoic chamber, the detail of the experiment and comparison between simulation and experimental results are shown in section IV. And in section V, the sound field distribution characteristics of three-phase filter capacitor are observed and then analyzed using the proposed model and BEM model respectively.

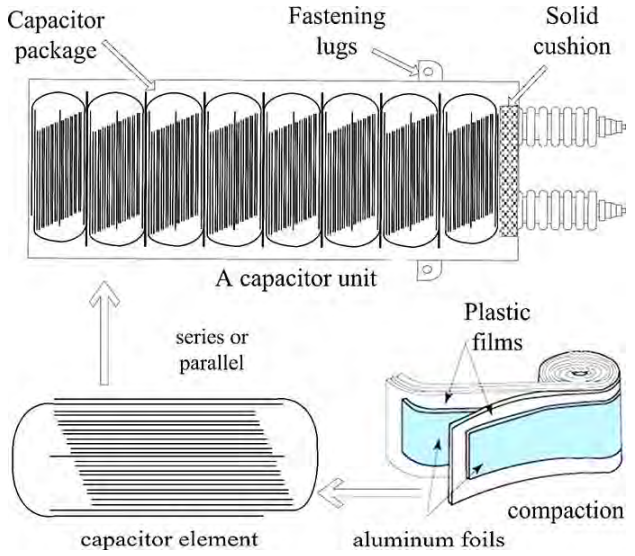

FIGURE 4. Structure of oil-immersed full-film capacitor.

II. THE MECHANISM OF FILTER CAPACITOR VIBRATION AND NOISE

The structure of the mostly used oil-immersed full-film capacitor is shown in Figure 4. One capacitor unit consists of several capacitor elements, which is compacted by plastic films and aluminum foils. The capacitor elements are connected in series or parallel. When the voltage waveform across the capacitor is distorted during the commutation procedure, a large number of harmonic voltage components bring high-frequency electrostatic force. When the frequency of the electrostatic force reaches or approaches the natural vibration frequency of the capacitor, the vibration and noise of the capacitor will be greatly strengthened.

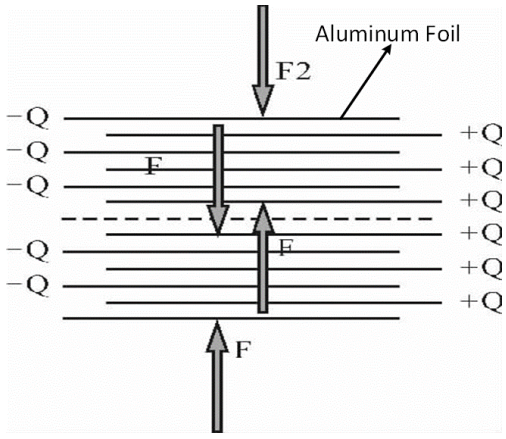

FIGURE 5. Schematic diagram of internal electrodes of capacitor elements.

Force analysis of aluminum foils gained from bipolar plate capacitor model is shown in Figure 5, where Q is the charge quality of aluminum foils, and F represents the electric force applied to the foils. According to the simplified capacitor bipolar plate model, electrostatic force between two plates of a capacitor can be obtained by

$$f = \frac{1}{2}\varepsilon AE^2 = \frac{1}{2d^2}\varepsilon Au^2 \tag{1}$$

where, ε is dielectric constant, A is area of plate, d is distance between two plates and u refers to voltage between the plates.

The electrostatic force between the plates is proportional to the square of the instantaneous value of the plate voltage, which indicates that the vibration noise of the capacitor caused by electrostatic force is proportional to the square of the voltage. According to the placement of capacitor element, it is clear that the vibration of the capacitor is mainly concentrated in the bottom-top direction. As a result, the noise is mainly radiated in this direction consistently.

For commonly used six-pulse converter, main components of filter capacitor vibration are concentrated at 500Hz, 700Hz, 1100Hz and 1300Hz. Noise with higher frequencies decays faster in air. That is to say, predicting the noise components with lower frequencies also greatly helps the control of the overall noise.

III. PROPOSED TRESM BASED ACOUSTIC MODEL FOR FILETER CAPACITOR

BEM is a traditional way to describe the sound field accurately, but it will consume a lot of computing resources. The reconstruction of three-phase filter capacitor sound field costs more than 24 hours. As for more equipment and larger areas, it is almost impossible. To simplify the solution procedure and to improve the simulation efficiency, TRESM is introduced.

A. PRINCIPLE OF THE EQUIVALENT SOURCE METHOD AND TIKHONOV REGULARIZATION

ESM use equivalent sources inside the surface boundary to replace the original source, as shown in Figure 6, and the

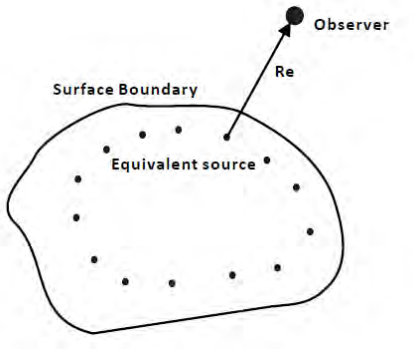

FIGURE 6. The equivalent source method.

wave measured by observer is actually the superposition of the sound field generated by all the monopoles [20]–[22].

Whether the reconstruction of the sound field is accurate enough directly depends on the accuracy of the monopole strength. Suppose there being N equivalent sources and M measuring points, then sound pressure measured at M points is

$$p = Gq \tag{2}$$

where, p is column vector composed of sound pressure values measured at M measuring points, q is column vector composed of strength of monopoles, and

$$p = (p_1, p_2, \cdots, p_m)^T \tag{3}$$
$$q = (q_1, q_2, \cdots, q_n)^T \tag{4}$$

G is the $M \times N$ transfer function matrix, to describe the relationship between the sound pressure value measured by M test points and the strength of N equivalent sources. Each element in G is recorded as $g(m, n)$, which means Transfer function between the mth measurement point and the nth equivalent source, $(0 < m \leq M, 0 < n \leq N)$, and

$$g(m, n) = i\rho ckg(r_m, r_n) \tag{5}$$

where:

ρ– Air density, usually $1.29Kg/m^3$,

c– Sound velocity in the air, usually $340m/s$,

k– Wave number,

$g(r_m, r_n)$– Green Function, expressed as:

$$g(r_m, r_n) = \frac{e^{-ik|r_m - r_n|}}{4\pi\,|r_m - r_n|} \tag{6}$$

r_m means the position vector of mth measuring point, r_n means the position vector of nth equivalent sources [23]–[25].

Usually, the number of equivalent sources is much larger, $M < N$, then (2) is actually an ill-condition equation. In this case, the solution of (2) is not unique [26], [27]. Then Tikhonov regularization method has to be introduced to minimize below function through several times of iteration [25], [28], [29]:

$$\|p - Gq\|_2^2 + \lambda^2 \|q\|_2^2 \tag{7}$$

λ is the regularization parameter.

B. REGULARIZATION BY GENERALIZED CROSS VALIDATION (GCV) METHOD

Regularization plays an important role in ill-posed morbid equation resolution, precision of regularization affects the accuracy of the equivalent source strength directly and significantly. Generalized cross validation (GCV) method, L-curve method and Hald Empirical Formula (HEF) method are often adopted to choose a better regularization parameter.

L-curve method determines the regularization parameter by finding the corner point and solving maximum curvature of the L-curve [30]. GCV method constructs a GCV function based on the error model and regularization solution [31]. In HEF method, a formula is directly used to determine the regularization parameter according to conditions already known. In [32], these three parameter determination methods are compared. L-curve method only works at low frequency (less than 2000Hz), GCV method has been observed to perform very well when frequency is lower than 3000Hz, the reconstruction results of HEF method is not very stable at low frequency, but it is more accurate at frequency higher than 3000Hz.

Taking precision and applicable frequency range into consideration, GCV method is the better choice to determine the regularization parameter.

The regularization parameter λ can be determined using:

$$\lambda = \frac{\|(C - I_m)P\|_2^2}{(Tr(I_m - C))^2} \tag{8}$$

I_m is the M-order unit matrix, Tr represents the trace of matrix, and matrix C is:

$$C = G(G^H G + \lambda I_n)^{-1} G^H \tag{9}$$

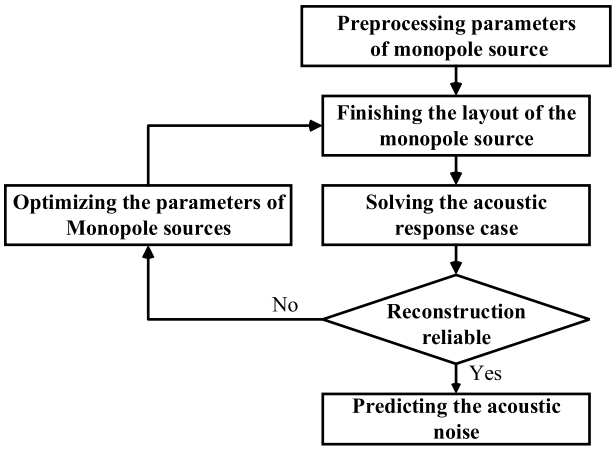

FIGURE 7. Optimization design procedure of monopole source equivalent model.

When the strength of the equivalent sources are properly chosen, the reconstruction of the sound field can theoretically be achieved, the optimization design procedure is shown in Figure 7.

C. PROPOSED TRESM FILTER CAPACITOR ACOUSTIC MODEL

Firstly, the number of monopole sources is determined. How to arrange those sources, especially to determine the number and location of point sources is really hard for ESM modeling, and arrangement of sources is obtained in many attempts. The monopole sources are placed at an envelope inside capacitor with scaling ratio 40%. Since the vibration is mainly concentrated on the frequency components lower than 1800Hz, which means the corresponding wavelength is larger than 180mm. For the target scaling model of length 380mm width 145mm and height 380mm, the distance between neighboring sources is finally set as 15mm, satisfying requirements that $d \leq \frac{1}{6}\lambda$. Thus 433 monopole sources are used and their position is determined. Schematic diagram of TRESM model is shown in Figure 8.

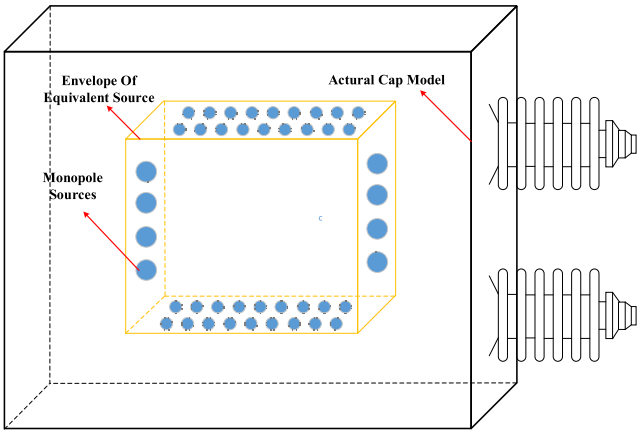

FIGURE 8. Schematic diagram of TRESM for filter capacitor.

Secondly, the monopole sources are arranged in Virtual. Lab, together with their strength solved by (2). It should be noted that strength of the sources needs to be transferred from sound pressure to sound intensity using the following equation [33]–[35].

$$I = \frac{p_a^2}{\rho_0 c_0} \tag{10}$$

where,

I– Sound intensity, kg/s^2

p_a– Amplitude of sound pressure, Pa

$\rho_0 c_0$– Acoustic impedance, $kg/m^2 \cdot s$

Then the acoustic response is solved in Virtual. Lab, using the source strength as boundary conditions, and whether the results are reliable is evaluated. If not satisfied with the reconstruction result, the regularization parameter can be adjusted finely to optimize the source strength through several times of iteration.

The established TRESM model in Virtual. Lab is shown in Figure.9, the bushings are ignored. And in Virtual. Lab, there is no capacitor any more, only a series of monopoles. To observe sound pressure cloud diagrams, three plane field point meshes are set, just as Figure.9(b) indicates. Three plane field meshes pass through the center of the model and are parallel to the broad side, narrow side and bottom of the TRESM model, respectively. A total reflection surface working as ground is set 990mm below TRESM model.

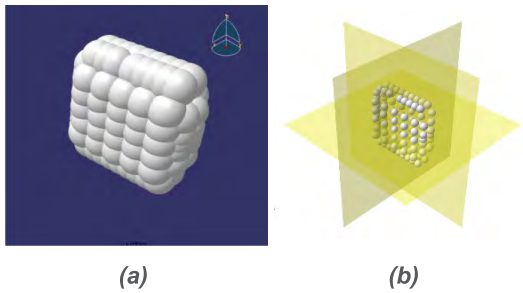

FIGURE 9. (a) Established TRESM model in virtual.Lab. (b) The schematic of noise simulation plane for TRESM model.

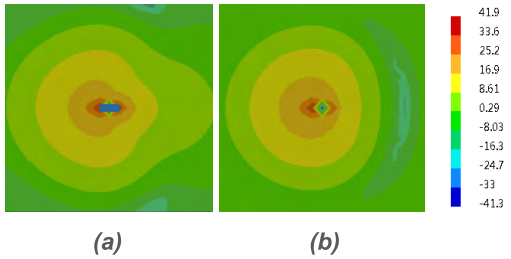

FIGURE 10. Sound pressure of (a) BEM and (b) TRESM at 200Hz.

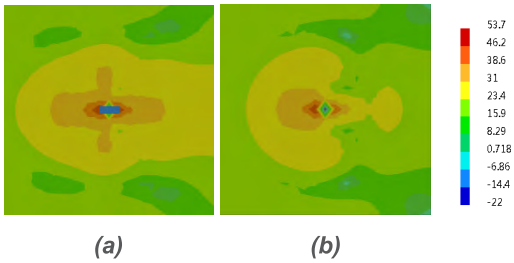

FIGURE 11. Sound pressure of (a) BEM and (b) TRESM at 500Hz.

D. COMPARISON OF THE RESULTS BY DIFFERENT MODELING METHOD

The TRESM solution frequency range is set to 100-2500Hz, with step 100Hz. Then the results are compared with those obtained by BEM model Under the same conditions, and analysis is done from the perspective of sound field characteristics and solution efficiency.

The reconstructed sound field are compared in the following Figure 10-Figure 15. The result is observed on a horizontal plane at different frequency. When frequency is low, at 200Hz for example, the sound field looks like that generated by single monopole source. With the increase of frequency, it is more obvious that acoustic noise near the bottom side becomes much stronger. And interference phenomenon between the various surfaces of the capacitor appears though still not very obvious for single capacitor. Comparing with simplified TREMS model, BEM model performs better when reflecting noise interference phenomenon, and interference

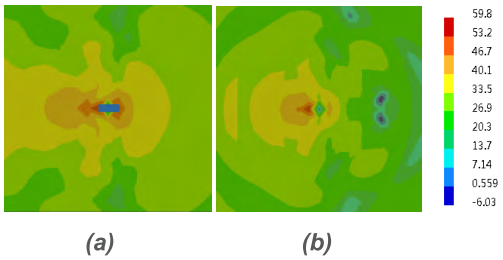

FIGURE 12. Sound pressure of (a) BEM and (b) TRESM at 900Hz.

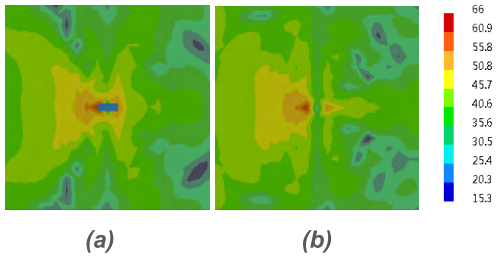

FIGURE 13. Sound pressure of (a) BEM and (b) TRESM at 1500Hz.

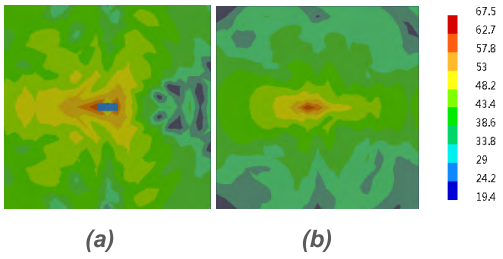

FIGURE 14. Sound pressure of (a) BEM and (b) TRESM at 1800Hz.

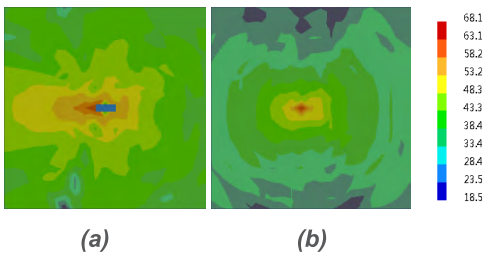

FIGURE 15. Sound pressure of (a) BEM and (b) TRESM at 2100Hz.

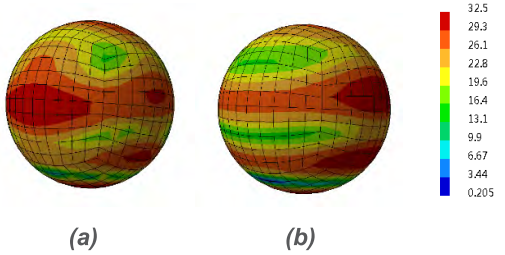

FIGURE 16. Sound pressure(dB) of (a) BEM and (b) TRESM at 500Hz.

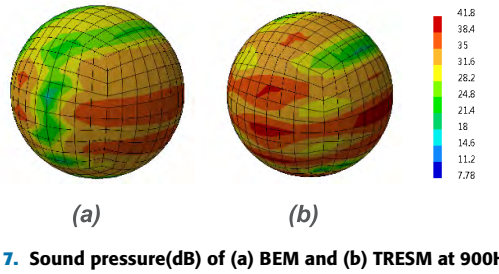

FIGURE 17. Sound pressure(dB) of (a) BEM and (b) TRESM at 900Hz.

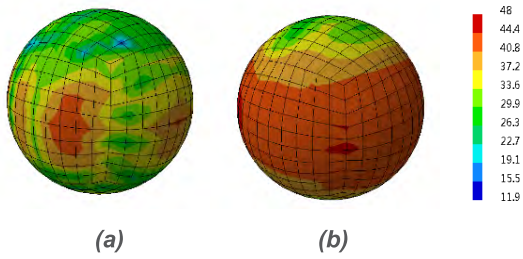

FIGURE 18. Sound pressure(dB) of (a) BEM and (b) TRESM at 1500Hz.

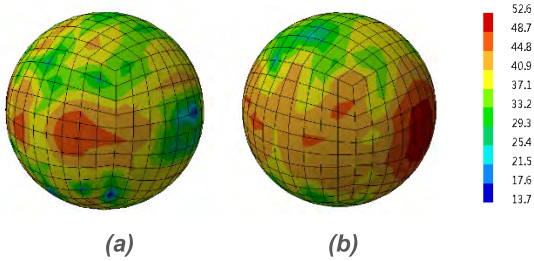

FIGURE 19. Sound pressure(dB) of (a) BEM and (b) TRESM at 1800Hz.

fringes is much clear near the normal direction of the broad side. But in general, the sound pressure deviation between the results of experiment and simulation are less than 4 dB, which means both the BEM and TRESM model are accurate and reliable.

Sound distribution is also observed on the spherical observation surface, shown in Figure 16-Figure 19. Similar to the plane distribution of sound pressure, when the frequency is relatively low (less than 1300Hz), the amplitude and distribution of the sound pressure on the spherical field obtained by two different methods are very close. Because ground could be regarded as an ideal reflective surface, the interference fringes formed between the model and the ground are more obvious. At higher frequencies, interference fringes generated by acoustic wave can be observed on the spherical surface, though this phenomenon is not as significant in TRESM model.

IV. CAPACITOR NOISE AND VIBRATION MEASUREMENT

In order to verify whether the equivalent source model is reliable, this paper makes an acoustic measurement of a filter capacitor in a semi-anechoic chamber. The experimental circuit is shown as Figure 20. The harmonic current with several components at different frequencies could be generated by the harmonic source. Then harmonic current flows through the reactor and is loaded on the capacitor finally. The reactor is used to compensate the power frequency current of capacitor unit. The circuit current and the voltage between the two capacitor terminals can be measured by the current sensor

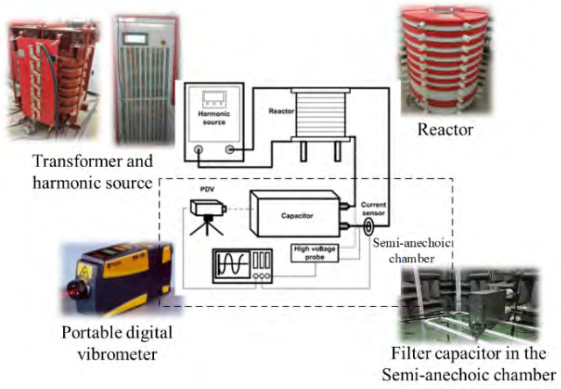

FIGURE 20. Experimental circuit.

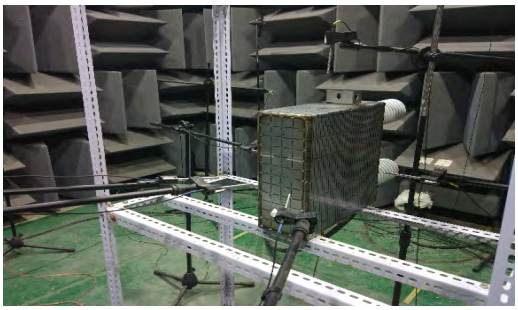

FIGURE 21. The capacitor scaling model.

and the high voltage probe, respectively. And the measurement results will be displayed on the oscilloscope. The PDV (Portable Digital Vibrometer) is used to determine the surface vibration, and we can also exchange it to sound pressure probe to get the sound pressure data in space. The tested capacitor and measuring equipment are in the semi-anechoic chamber, while the source and reactor are outside to avoid interference.

In general, the size and capacity of the filter capacitor device in the HVDC converter station is very large, which makes it difficult to set up and experiment directly in the laboratory. Then a scaling model of length 380mm width 145mm and height 380mm is used, as shown in Figure.21. The model is identical to the actual capacitor used in converter station, but the reactive capacity is 134kvar, which is much smaller. The capacitor is put at the height of 800mm.

According to GB/T 32524, 17 measurement points are located on the envelope surface 1000 mm away from the surface of the capacitor. To improve the measurement accuracy, 36 spatial measurement points are used, which are located on the same envelope surface. Sound pressure level are measured at the points set according to GB/T 32524, results are shown in figure 22.

It is obvious that the results of simulation are always 2∼4dB lower than the experimental results, this could be explained by the loss of the information when the discrete vibration information is applied as boundary condition. When more intensive measuring points are set, the results will be more accurate.

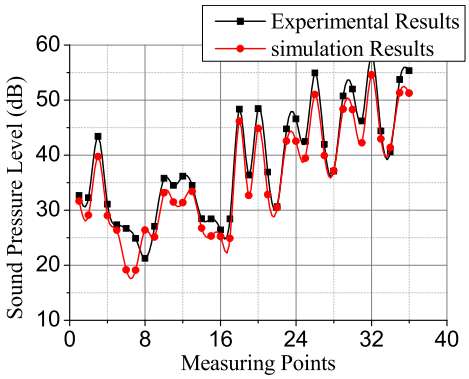

FIGURE 22. Sound pressure level gained through experiment and simulation.

TABLE 1. The deviation between the experimental result and simulation results (at 1000Hz).

Point Number	Deviation (TRESM)/dB	Deviation (BEM)/dB
1	0.691	1.045
4	2.093	2.091
7	3.195	5.784
10	2.675	2.653
13	1.055	1.083
16	5.031	1.204
19	3.580	3.703
22	0.354	0.168
25	4.362	3.056
28	1.192	0.075
31	3.172	3.940
34	0.527	0.796

And the deviation between the experimental result and simulation results gained by BEM and TRESM models are displayed in TABLE 1, respectively. From the table, it is indicated that though the measurement error of the TRESM model is larger at some measurement points, the results obtained by the two methods are very close for most of the measurement points.

V. SOUND FIELD RECONSTRUCTION OF THREE-PHASE FILTER CAPACITOR

For converter station, the filtering equipment is arranged in groups, and the same three-phase filtering device exists in each group. Then it is usually unrealistic to obtain the filter capacitor sound field by the sound pressure measurement method because of the complex acoustic environment and transmission power fluctuations. As a result, simulation has become an often-used method to acquire the sound field characteristics of the filter capacitors. Taking the phase difference between the three-phase power supplies into account, the actual vibration of capacitor in different phase will also have a 120° phase difference, so the phase sequence of voltage and capacitor surface vibration should be determined first. According to [36], for a three-phase positive sequence voltage, the square of the voltage is negative sequence. According to the capacitor vibration system model, the vibration of the capacitor casing is proportional to the square of the

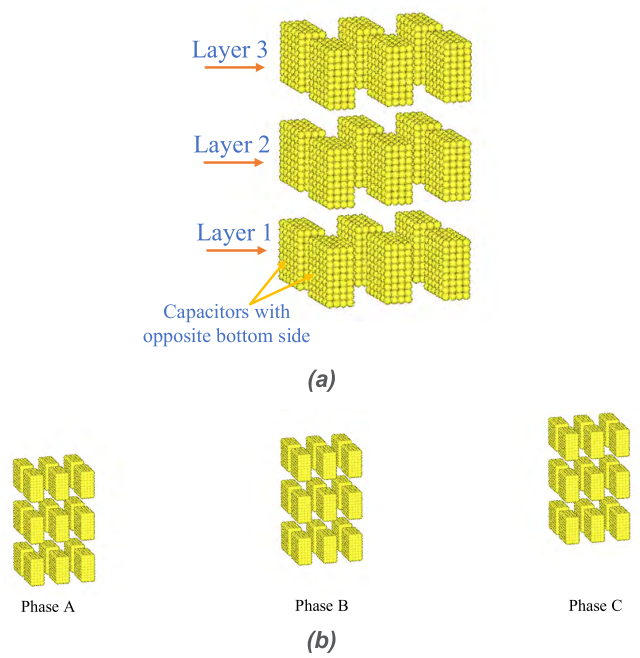

FIGURE 23. TRESM model of three-phase filter capacitor. (a) Single phase arrangement, (b) Three-phase arrangement.

voltage, so the vibration phase of the capacitor is also negative sequence, but if the three-phase voltage is negative sequence, things are exactly opposite.

In this paper, the vibration phase of the capacitor is corrected under the positive sequence voltage, and the capacitor is placed in the vertical position with broad side of the different phase capacitors parallel, as shown in Figure 23. In this case, 54 capacitors are used. One phase contains 3 layers, and 6 capacitors every layer. The distance between broad side of the neighboring capacitor is 150mm, and that between phases is much larger, 1600mm is used in this acoustic case.

The results at different frequencies are shown in Figure 24-Figure 28. Sound field is observed from three different direction, and the observation surfaces should not be placed too close to the capacitor, otherwise the effects of vibration noise from other surfaces will be ignorable within the observation range. Then the horizontal plane is set at the height of human ear, and the other two planes are 1000mm away.

From the sound field distribution, the sound field of the three-phase capacitors is apparently asymmetrical. For example, acoustic noise is stronger near phase A at 700Hz, but that is much weaker near phase A at 1800Hz and acoustic far field radiation is concentrated in the 135° and 225° direction, which means the noise is concentrated in a certain direction or a certain phase, and the directivity of the sound field changes with frequency.

Due to the interaction of the sound fields generated by each surface of the capacitor, the sound field may converge at some location away from the capacitor, causing that sound

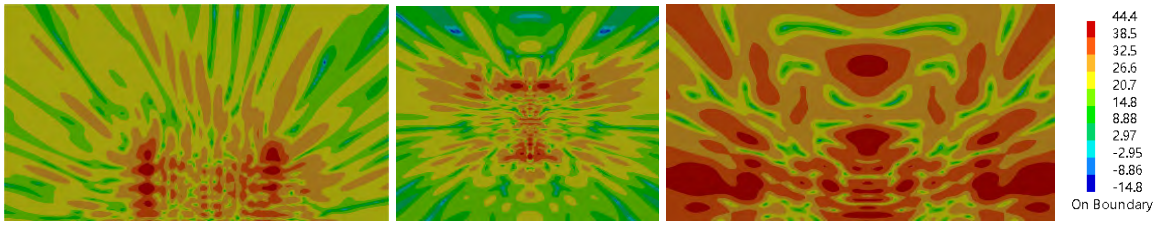

FIGURE 24. Sound pressure(dB) distribution on the observation surfaces at 700Hz.

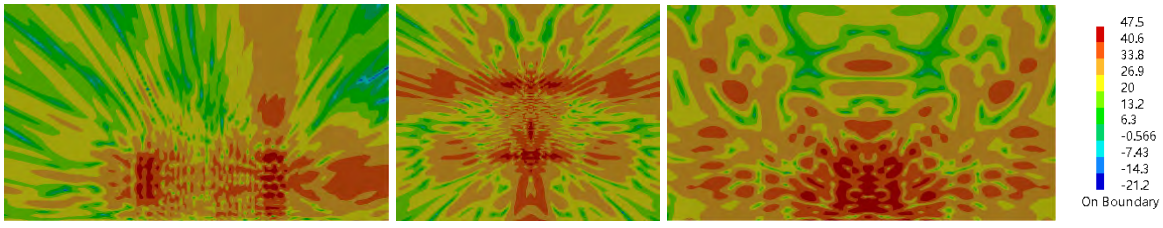

FIGURE 25. Sound pressure(dB) distribution on the observation surfaces at 1000Hz.

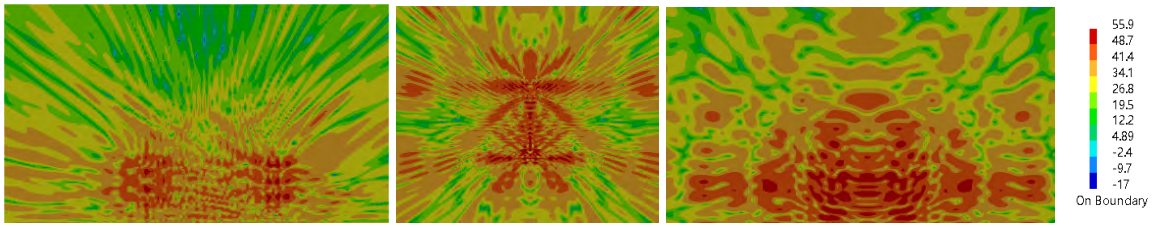

FIGURE 26. Sound pressure(dB) distribution on the observation surfaces at 1400Hz.

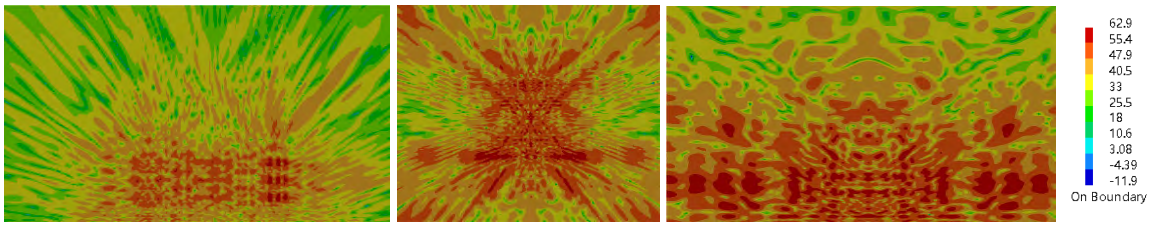

FIGURE 27. Sound pressure(dB) distribution on the observation surfaces at 1800Hz.

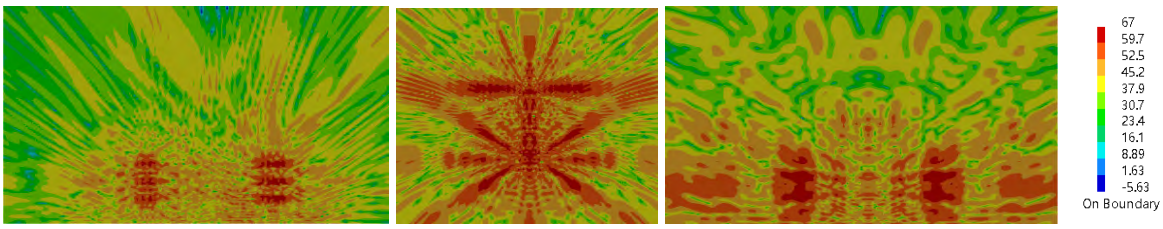

FIGURE 28. Sound pressure(dB) distribution on the observation surfaces at 2000Hz.

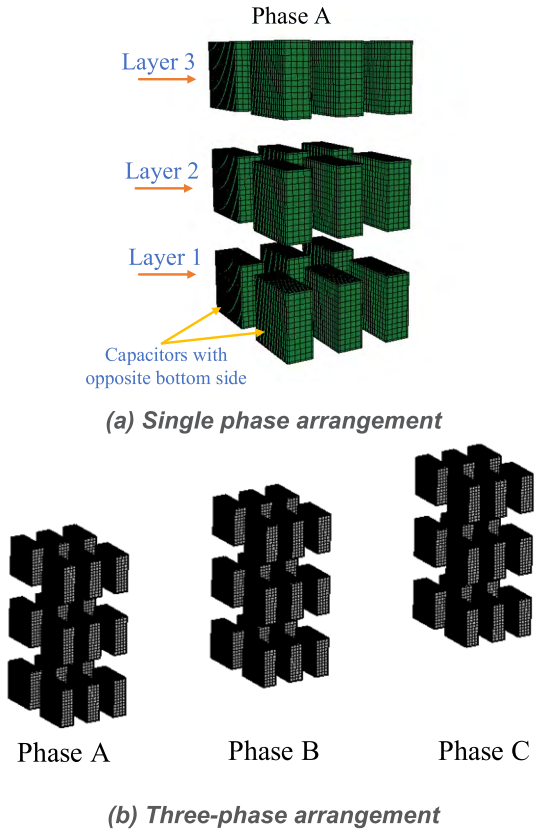

FIGURE 29. BEM model three-phase filter capacitor.

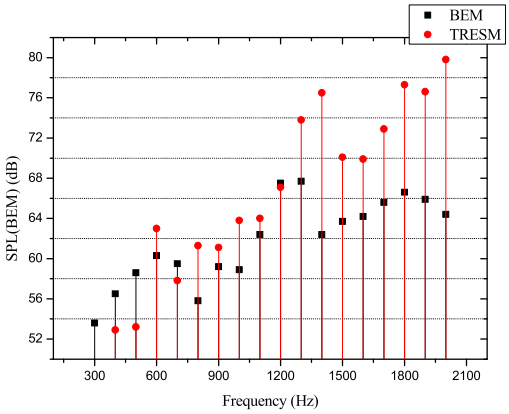

FIGURE 30. Sound pressure level gained through simulations.

pressure amplitude suddenly becomes larger, and it is usually more common at lower frequencies. This could partly explain why in some cases, the noise measured at the boundary of the converter station meets the standard, but the noise measured outside the station is stronger.

With the increase of frequency, the wavelength of the acoustic wave decreases, and the interference fringes are increasingly intensive. The higher the frequency, the faster the attenuation of far-field radiation, the more obvious the directivity of the sound field distribution.

The three-phase sound field is also simulated with the BEM model as shown in Figure 29 and compared with the results obtained by the TRESM. Figure 30 shows sound pressure amplitude at different frequencies. The amplitude of sound pressure increases together with the frequency.

Because the harmonics are main components of harmonics generated by the six-pulse converter, it is not strange that sound pressure amplitude is much higher at 500Hz and 1300Hz, this is consistent with the actual situation. When the frequency is lower than 1300Hz, the amplitude of the sound pressure obtained by the two methods is close, when the frequency is higher, the amplitude error is significantly increased. Considering that the wavelength is short when the frequency is high, the performance of TRESM in terms of acoustic interference is weaker in single capacitor, therefore, in the sound field simulation of multiple capacitors, the accuracy of the TRESM method needs to be further improved.

For each of the various modeling methods mentioned, their respective advantages and disadvantages are

TABLE 2. Advantages and disadvantages of TRESM, BEM and traditional ESM.

Algorithms	Solution Efficiency	Computer Memory occupied	Low-Frequency Prediction	Middle-Frequency Prediction	High-Frequency Prediction
TRESM	★★★★	★★★★	★★★☆	★★	★
BEM	★	★	★★★★	★★★★	★★★☆
Traditional ESM	★★★☆	★★★★	★★★	★	★

TABLE 3. Solution time of TRESM, BEM and traditional ESM.

Algorithms	Single Capacitor	Single Phase with 8 Capacitors	Three Phases with 54 Capacitors
TRESM	1.6s	14.1s	5.2min
BEM	17.3s	228.3s	>3600min
Traditional ESM	2.0s	18.2s	7.4min

comprehensively compared in the TABLE 2 and specific solution time of these methods are also given in table 3. BEM models are more accurate at different frequencies but are of worse efficiency and require more computing resources. TRESM is highly efficient, and accuracy is pretty good at lower frequencies, but still needs improvement at higher frequencies.

VI. CONCLUSION

In this paper, a TRESM filter capacitor acoustic model is proposed, it is a great simplification of the original acoustic model. The noise and surface vibration of the scaling capacitor is measured in a semi-anechoic chamber, the accuracy of the proposed model is verified. And comparison between the reconstructed sound field by BEM model and TRESM has been made, it can be found that the simulation results of sound pressure level are always 2∼4 dB lower than the experimental data, but the characteristic of noise distribution can be accurately presented. The solution time can be reduced significantly when using the TRESM model. TRESM model can obtain fairly reliable simulation results when the equivalent source strength is chosen appropriately, though the TRESM model still needs further improvement in terms of sound field interference. And sound field distribution of three-phase filter capacitor is observed using the TRESM model and BEM model respectively. The sound field of the three-phase capacitors is apparently asymmetrical. With the increase of frequency, the amplitude of sound pressure increases and the interference fringes are increasingly intensive. And when frequency is lower than 1300Hz, sound pressure level gained by TRESM filter capacitor model is more reliable. This newly proposed method has not yet been applied in industrial practice widely, but with the continuous optimization of the method, the reliability and simplicity of this method will be further improved. It is anticipated the proposed TRESM based model will be used in the future industrial HVDC application.

REFERENCES

[1] W. Ping and G. Wei, "Analysis on the current situation of electricity and energy in China and its solution," *Elect. Eng.*, vol. 13, no. 5, pp. 1–5, 2018.

[2] M. Weimin and F. Jichao, "Planning and design of UHVDC transmission system," *High Voltage Eng.*, vol. 14, no. 8, pp. 2545–2549, 2015.

[3] Z. Yong and H. Haoyu, "Harmonics of HVDC transmission system and its suppression," *Telecom World.*, vol. 14, no. 10, pp. 218–220, 2016.

[4] *High Voltage Direct Current (HVDC) Substation Audible Noise*, Standard IEC-TS61973, 2012.

[5] G. Lin, L. Fuyun, and F. Chunlin, "Audible noise study of power capacitor," *Power Capacitor Reactive Power Compensation*, vol. 36, no. 1, pp. 1–6, 2015.

[6] J. Shengchang, Z. Lingyu, and C. Hantao, "Review and prospect on audible noise of HVDC filter capacitors," *Power Capacitor Reactive Power Compensation*, vol. 38, no. 4, pp. 1–10, 2017.

[7] M. D. Cox and H. H. Guan, "Vibration and audible noise of capacitors subjected to nonsinusoidal waveforms," *IEEE Trans. Power Delivery.*, vol. 9, no. 2, pp. 856–862, Apr. 1994.

[8] Y. Kening, "Generation mechanism and characteristics analysis of power capacitor noise," *Power Capacitor Reactive Power Compensation*, vol. 16, no. 3, pp. 10–13, 1995.

[9] C. Xin, "Experimental modal analysis on AC-filter capacitor in HVDC converter station," M.S. thesis, Dept. Mech. Manuf. Automat., Hefei Univ. Technol., Hefei, China, 2012.

[10] M. Hurkala, "Study on vibartion characteristics of power capacitor under different excitation modes," *Power Capacitor Reactive Power Compensation*, vol. 33, no. 5, pp. 53–58, 2012.

[11] H. Marcin, "Noise analysis of high voltage capacitors and dry-type air-core reactors," M.S. thesis, Dept. Elect., Aalto Univ., Helsinki, Finland, 2013.

[12] L. Zhu, J. Li, Y. Shi, H. Rehman, and S. Ji, "Audible noise characteristics of filter capacitors used in HVDC converter stations," *IEEE Trans. Power Del.*, vol. 32, no. 5, pp. 2263–2271, Oct. 2017.

[13] W. Peng, J. Shengchang, L. Yanming, and C. Tao, "Study on an audible noise reduction measure for filter capacitors based on compressible space absorber," *IEEE Trans. Power Del.*, vol. 26, no. 1, pp. 438–445, Jan. 2011.

[14] G. Lin, "Research on key technologies of power capacitor noise control," M.S. thesis, Dept. Mech. Eng., Guilin Univ. Electron. Technol., Guilin, China, 2015.

[15] W. Haozheng, "Research on audible noise predicting system of HVDC transmission," Ph.D. dissertation, Dept. Mech. Des. Theory., Hefei Univ. Technol., Hefei, China, 2010.

[16] A. N. Tikhonov, "Solution of incorrectly formulated problems and the regularization method," *Soviet Math.*, vol. 4, no. 4, pp. 1035–1038, 1963.

[17] A. Pereira and Q. Leclere, "Improving the equivalent source method for noise source identification in enclosed spaces," in *Proc. 18th Int. Congr. Sound Vib.*, Rio de Janeiro, Brazil, 2011, pp. 2690–2697.

[18] A. Pereira, Q. Leclère, L. Lamotte, S. Paillasseur, and L. Bleandonu, "Noise source identification in a vehicle cabin using an iterative weighted approach to the ESM method," in *Proc. 25th Int. Conf. Noise Vib. Eng.*, Leuven, Belgium, 2012, pp. 17–19.

[19] S. Gade, J. Hald, and K. B. Ginn, "Wideband acoustical holography," in *Proc. 43rd Int. Congr. Noise Control Eng., Improving World through Noise Control*, Melbourne. Australia, Apr. 2014, p. 9.

[20] R. Jeans and I. C. Mathews, "The wave superposition method as a robust technique for computing acoustic fields," *J. Acoust. Soc. Amer.*, vol. 92, no. 2, pp. 1156–1166, Jun. 1998.

[21] S. Lee, "Review: The use of equivalent source method in computational acoustics," *J. Comput. Acoustics.*, vol. 25, no. 1, Mar. 2017, Art. no. 1630001.

[22] R. Madoliat, N. M. Nouri, and A. Rahrovi, "Equalization of acoustic source using multi-pole sources and source strength estimation using inverse method," *Appl. Acoustics.*, vol. 113, pp. 210–220, Dec. 2016.
[23] S. Lee, S. Kenneth, S. Brentner, and P. J. Morris, "Assessment of time-domain equivalent source method for acoustic scattering," *AIAA J.*, vol. 49, no. 9, pp. 1897–1906, 2011.
[24] M. E. Sequeira and V. H. Cortínez, "Optimal acoustic design of multi-source industrial buildings by means of a simplified acoustic diffusion model," *Appl. Acoustics.*, vol. 103, pp. 71–81, Feb. 2016.
[25] J. B. Fahnline, "Solving transient acoustic boundary value problems with equivalent sources using a lumped parameter approach," *Acoust. Soc. Amer.*, vol. 140, no. 6, pp. 4115–4129, Dec. 2016.
[26] H. J. Kim, K. Choi, H. B. Lee, H. K. Jung, and S. Y. Hahn, "A new algorithm for solving ill conditioned linear systems," *IEEE Trans. Magn.*, vol. 32, no. 3, pp. 1373–1376, May 1996.
[27] D. Chaniotis and M. A. Pai, "Iterative solver techniques in the dynamic simulation of power systems," in *Proc. IEEE Power Eng. Soc. Summer Meeting*, Jul. 2000, pp. 609–613.
[28] A. Pereira, Q. Leclère, and J. Antoni, "A theoretical and experimental comparison of the equivalent source method and a Bayesian approach to noise source identification," in *Proc. 4th Berlin Beamforming Conf.*, Perlin, GER, Feb. 2012, pp. 22–23.
[29] G. Ping, Z. Chu, and Z. Xu, "A refined wideband acoustical holography based on equivalent source method," *Sci. Rep.*, vol. 7, Mar. 2017, Art. no. 43458.
[30] P. C. Hansen and D. P. O'Leary, "The use of L-curve in the regularization of discrete ill-posed problems," *SIAM J. Sci. Comput.*, vol. 14, no. 6, pp. 1487–1503, 1993.
[31] M. A. Lukas, "Robust GCV choice of the regularization parameter for correlated data.," *J. Integral Equ. Appl.*, vol. 22, no. 3, pp. 519–547, 2010.
[32] Z. Chu, G. Ping, and Y. Yang, "Determination of regularization parameters in near-field acoustical holography based on equivalent source method," *J. Vibroeng.*, vol. 17, no. 5, pp. 2304–2313, Aug. 2015.
[33] D. Gonghuan and Z. Zhemin, *Acoustic Basis*. Nanjing, China: Nanjing Univ. Press, 2012, pp. 125–130.
[34] X. Ruan and H. Wei, "Model for predicting outdoor coherent noise and its engineering application," *China Environ. Sci.*, Vol. 35, no. 6, pp. 1877–1884, 2015.
[35] C. Bi, W. Jing, and Y. Zhang, "Reconstruction of the sound field above a reflecting plane," *J. Sound Vibrat.*, vol. 386, pp. 149–162, Jan. 2017.
[36] Z. Lingyu, "Study on Noise Prediction Technology and Reduction Measures for AC Filter Capacitor Installations in Converter Stations," Ph.D. dissertation, Dept. Elect. Eng., Xi'an Jiaotong Univ., Xi'an, China, 2014.

RUI WANG received the B.S. degree in electrical engineering from Xi'an Jiaotong University, Xi'an, China, in 2017, where he is currently pursuing the M.S. degree in power electronics with the School of Electrical Engineering. His research interests include sound field optimization and active noise reduction technology for the filtering field of converter station.

WENJIE CHEN received the B.S., M.S., and Ph.D. degrees in electrical engineering from Xi'an Jiaotong University, Xi'an, China, in 1996, 2002, and 2006, respectively. Since 2002, she has been a Member of the Faculty of the School of Electrical Engineering, Xi'an Jiaotong University, where she is currently a Professor. From 2012 to 2013, she was with the Department of Electrical Engineering and Computer Science, The University of Tennessee, Knoxville, TN, USA, as a Visiting Scholar. She then came back to Xi'an Jiaotong University, and engaged in the teaching and researches in power electronics. Her main research interests include electromagnetic interference, active filters, and power electronic integration.

LINGYU ZHU (M'16) was born in Shandong, China, in 1988. He received the B.S. and Ph.D. degrees in electrical engineering from Xi'an Jiaotong University, China, in 2009 and 2014, respectively, where he is currently an Associate Professor. His research interests include condition monitoring and vibration characteristics of power equipment.

SHENGCHANG JI was born in Shandong, China, in 1976. He received the B.S. and Ph.D. degrees in electrical engineering from Xi'an Jiaotong University (XJTU), Xi'an, China, in 1998 and 2003, respectively. From 2004 to 2006, he was a Postdoctoral Researcher with the China XD Group, Shaanxi, Xi'an. From 2010 to 2011, he was a Visiting Scholar with the High Voltage and Power Electronic Laboratory, The Ohio State University. He is currently a Professor with Xi'an Jiaotong University. His research work covers vibration and noise of power equipment, dielectric phenomena of high voltage insulation, and condition maintenance of power equipment.

XIAOTENG LI received the M.S. degree in electrical engineering from Xi'an Jiaotong University, Xi'an, China, in 2007. Since 2007, she has been a Member of the State Grid Shaanxi Electric Power Research Institute, where she is currently a Senior Engineer. She is engaged in the research of the stability of power system.

LIYU DAI received the B.S. degree in electrical engineering from Fuzhou University, Fuzhou, China, in 2017. He is currently pursuing the M.S. degree in power electronics with the School of Electrical Engineering, Xi'an Jiaotong University. His research interests include electromagnetic interference and active filters.

YANG YANG received the B.S. degree in electrical engineering from Nanjing Agricultural University, Nanjing, Jiangsu, China, in 2017. She is currently pursuing the M.S. degree with Xi'an Jiaotong University, Xi'an, Shaanxi, China. Her current research interests include wireless power transfer and electromagnetic interference.